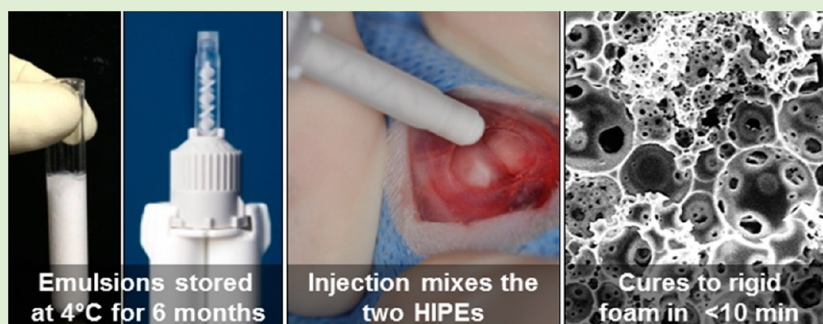


Injectable Polymerized High Internal Phase Emulsions with Rapid *in Situ* Curing

Robert S. Moglia, Michael Whitely, Prachi Dhavalikar,[†] Jennifer Robinson, Hannah Pearce, Megan Brooks, Melissa Stuebben, Nicole Cordner, and Elizabeth Cosgriff-Hernandez*

Department of Biomedical Engineering, Texas A&M University, College Station, Texas 77843-3120, United States



ABSTRACT: Polymerized high internal phase emulsions (polyHIPEs) have been utilized in the creation of injectable scaffolds that cure *in situ* to fill irregular bone defects and potentially improve tissue healing. Previously, thermally initiated scaffolds required hours to cure, which diminished the potential for clinical translation. Here, a double-barrel syringe system for fabricating redox-initiated polyHIPEs with dramatically shortened cure times upon injection was demonstrated with three methacrylated macromers. The polyHIPE cure time, compressive properties, and pore architecture were investigated with respect to redox initiator chemistry and concentration. Increased concentrations of redox initiators reduced cure times from hours to minutes and increased the compressive modulus and strength without compromising the pore architecture. Additionally, storage of the uncured emulsion at reduced temperatures for 6 months was shown to have minimal effects on the resulting graft properties. These studies indicate that the uncured emulsions can be stored in the clinic until they are needed and then rapidly cured after injection to rigid, high-porosity scaffolds. In summary, we have improved upon current methods of generating injectable polyHIPE grafts to meet translational design goals of long storage times and rapid curing (<15 min) without sacrificing porosity or mechanical properties.

INTRODUCTION

Emerging fields like tissue engineering are driving the development of novel materials with specialized properties to serve as temporary three-dimensional matrices to regenerate complex tissues.¹ Material chemistry and physical architecture are critical to guiding regeneration. An interconnected porous structure is needed to encourage cell growth, nutrient and metabolic waste transport, and neovascularization.² Bone and other structural tissues also require that these porous scaffolds have adequate mechanical properties to withstand physiological loading until tissue function is restored.^{1,3} Great effort has been spent developing materials and fabrication strategies to meet these design criteria; however, matching the constraints of tissue regeneration and sufficient mechanical properties to restore function remains challenging given that many of these properties are inversely related to each other. For example, high porosity enhances mass transport to support cell viability but typically reduces mechanical properties. Polymerized high internal phase emulsions (polyHIPEs) constitute a more recent scaffold fabrication technique that offers unique advantages in meeting these diverse criteria.⁴

PolyHIPEs have been investigated as tissue-engineered scaffolds because of their tunable mechanical properties and pore architectures that are appropriate for tissue regeneration.^{4–7} A unique advantage of the polyHIPEs developed in our lab is their solvent-free fabrication and low cure temperature that permits their use as an injectable scaffold that cures to rigid foams in the body. This injectability allows these scaffolds to match irregular defect geometries and thus eliminate gaps and micromotion, which could reduce the frequency of graft failure and revision surgeries.^{1,3,7} An injectable graft that cures *in situ* would also reduce the cost and time associated with computer-aided design and fabrication methods.⁸ Finally, the solvent-free fabrication method permits incorporation of bioactive cues to facilitate cell differentiation and promote new tissue growth.^{2,8}

While these scaffolds offer many advantages over alternative bone grafts, current biodegradable formulations require roughly 2 h to cure at body temperature.^{5,7} Clinicians prefer fast-curing

Received: February 18, 2014

Revised: July 9, 2014

Published: July 9, 2014

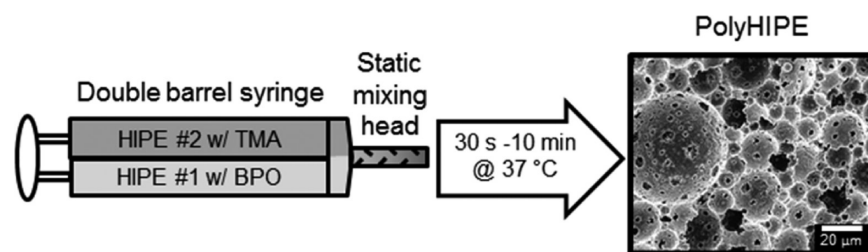


Figure 1. Schematic of the double-barrel syringe system.

materials that reduce surgical times, lower the patient's risk of infection, and rapidly stabilize defects.³ Poly(methyl methacrylate) (PMMA) bone cement cures in just 15 min and is the most common injectable system used clinically to stabilize orthopedic implants. Although PMMA bone cements are fast and direct, it does not facilitate tissue regeneration because it is highly exothermic, nondegradable, and nonporous. In contrast, an injectable polyHIPE that cures within 15 min would be advantageous because it can stabilize the defect and be loaded with cells prior to injection to provide a temporary matrix that supports tissue regeneration. In addition to rapid cure times, off-the-shelf grafts are preferred to allow use in both emergency and scheduled procedures.³ Thus, polyHIPE grafts must remain stable in storage for a minimum of 6 months and then cure rapidly after injection to facilitate clinical translation.

Previous iterations of injectable polyHIPE scaffolds relied on thermal initiation, the rate of which increases exponentially with temperature. A graft that cures *in situ* is constrained to a physiological cure temperature of 37 °C, well below the typical use temperatures of most thermal initiators. In this study, thermal initiation was replaced with a redox initiator system to decrease the set time of the HIPEs. Previous redox-cured polyHIPEs displayed enhanced cure rates but were not designed for biomedical use and often contained toxic or nondegradable components.^{9,10} Here, a method is described that allows for the fabrication of injectable polyHIPEs from biodegradable macromers that can be stored for months at a time and then rapidly cures *in situ*. This proposed method involves making two separate but nearly identical HIPEs: the first with an oxidizing initiator and the second with a reducing agent. Redox-paired initiators allow for rapid polymerization at low temperatures, while the use of a double-barrel syringe keeps the components separate and unpolymerized until the two components are mixed upon injection via a static mixing head. Via the careful selection of initiator concentrations, this system has the potential to permit stable storage of the uncured emulsion and rapid curing after injection into the defect. To this end, we investigated the effect of redox initiator concentration on the polyHIPE properties of three materials: ethylene glycol dimethacrylate (EGDMA), butanediol dimethacrylate (BDMA), and propylene fumarate dimethacrylate (PFDMA). The effects of redox concentration and ratio on cure time, pore architecture, and compressive modulus and strength were evaluated in relation to their use in orthopedic applications. Overall, these studies demonstrate the potential of this new method of fabricating rapid-curing polyHIPEs with long shelf lives for use as tissue-engineered bone grafts.

MATERIALS AND METHODS

Materials. Polyglycerol polyricinoleate (PGPR 4125) was donated by Paalsgard. All other chemicals were purchased and used as received from Sigma-Aldrich unless otherwise noted. Human mesenchymal

stem cells (hMSCs) were provided by the Texas A&M Health Science Center College of Medicine Institute for Regenerative Medicine at Scott & White.

PFDMA Synthesis. PFDMA was synthesized in a two-step process adapted from ref 11. First, propylene oxide was added dropwise to a solution of fumaric acid and pyridine in 2-butanone (2.3:1.0:0.033 molar ratio) and refluxed at 75 °C for 18 h. Residual propylene oxide and 2-butanone were removed by distillation, and the product was redissolved in dichloromethane. Residual acidic byproducts and water were removed with washing, and the product was dried under vacuum to yield the diester bis(1,2-hydroxypropyl) fumarate product. The diester was then end-capped with methacrylate groups using methacryloyl chloride in the presence of triethylamine. The diester:methacryloyl chloride:triethylamine molar ratio was 1:2.1:2.1. Hydroquinone was added to the diester to inhibit cross-linking during synthesis at a molar ratio of 0.008:1. The reaction mixture was kept below -10 °C to reduce undesirable side reactions and stirred vigorously under a nitrogen blanket. The macromer was neutralized overnight with 2 M potassium carbonate. Residual triethylamine and methacrylic acid were removed with an aluminum oxide column (7:1 Al₂O₃:TEA). The integration ratio of methacrylate protons to fumarate protons in the ¹H nuclear magnetic resonance spectra was used to confirm >90% functionalization for all macromers prior to polyHIPE fabrication: ¹H NMR (300 MHz, CdCl₂) δ 1.33 (dd, 3H, CH₃), 1.92 (s, 3H, CH₃), 4.20 (m, 2H, -CH₂-), 5.30 (m, 1H, -CH-), 5.58 (s, 1H, -C=CH₂), 6.10 (s, 1H, -C=CH₂), 6.84 (m, 2H, -CH=CH-).

Removal of Inhibitors by EGDMA and BDMA. EGDMA and BDMA, purchased from Sigma-Aldrich, were purified to remove inhibitors prior to use. The macromers were filtered through an aluminum oxide column to remove monomethyl ether hydroquinone. The purified products were stored at 4 °C under a nitrogen blanket until they were used for HIPE fabrication.

PolyHIPE Fabrication. HIPEs were fabricated using a model DAC 150 FVZ-K FlackTek Speedmixer according to a protocol adapted from ref 5. Briefly, the macromer was mixed with 10 wt % PGPR 4125 and a varied amount of benzoyl peroxide (0.5–5.0 wt %) prior to emulsification. A second mixture consisting of macromer, 10 wt % PGPR, and a varied amount of trimethylaniline (TMA, 0.5–5.0 wt %) was also combined prior to emulsification. Once both had been thoroughly mixed, an aqueous solution of calcium chloride (1 wt %) was then added to the organic phases [75% (v)] in three additions and mixed at 500 rpm for 2.5 min each. HIPEs were placed in a double-barrel syringe and the two components mixed upon injection using a static mixing head (1:1 ratio, 5 mL syringe with a 3 cm straight mixer, Sulzer Mixpac K-System). HIPEs were then placed in a 37 °C bath to initiate polymerization (Figure 1). PolyHIPE porosity is dictated by the initial aqueous volume fraction of the HIPE because of minimal shrinkage during curing. For this study, the volume fraction and corollary porosity were maintained at ~75%.

Rheological Analysis. The polyHIPE cure time was characterized using an Anton Paar MCR 301 rheometer based on a process adapted from ref 12. HIPEs were injected through a mixing head to facilitate redox initiation directly onto the 37 °C plate. Storage and loss moduli were measured every 15 s using a parallel-plate configuration with a 1 mm gap and 0.5% strain. The work time is presented as the onset of increasing storage modulus, and the set time is presented as the tan δ minimum, which corresponds to storage modulus yielding.

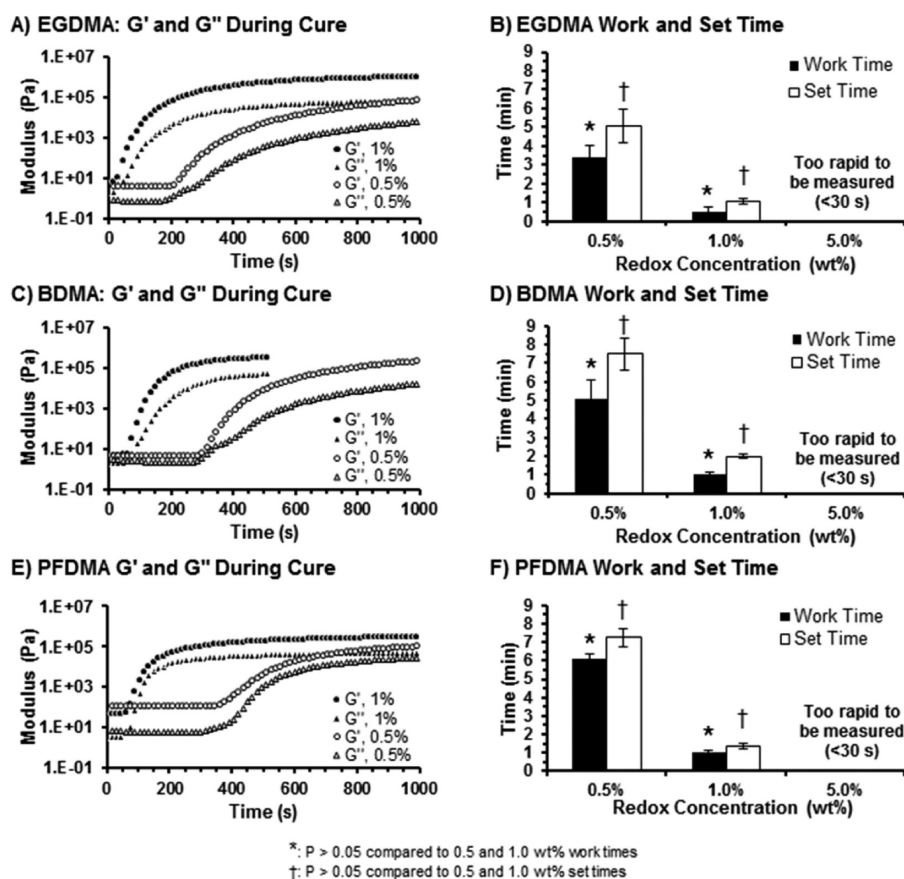


Figure 2. Storage and loss moduli during polymerization of EGDMA (A), BDMA (C), and PFDMA (E) polyHIPE and work and set times for EGDMA (B), BDMA (D), and PFDMA (F) polyHIPEs at 37 °C with a 1.0:1.0 TMA:BPO ratio.

Scanning Electron Microscopy. PolyHIPEs were dried *in vacuo* for 24 h to remove water prior to characterization of the pore architecture. The average pore and interconnect size of each composition were determined using scanning electron microscopy (SEM) (JEOL 6500). Circular specimens from three separate polyHIPE specimens were sectioned into quarters and fractured at the center. Each specimen was coated with gold and imaged in a raster pattern yielding five images. Pore size measurements were completed on the first 10 pores that crossed the median of each 500 \times magnification micrograph. Average pore sizes for each polyHIPE composition are reported ($n = 450$). A statistical correction was calculated to account for the random fracture plane through spherical voids and pores, $2/\sqrt{3}$.¹³ Average diameter values were multiplied by this correction factor, resulting in a more accurate description of the pore diameter.

Mechanical Testing. PolyHIPE compressive properties were measured using an Instron 3300 instrument equipped with a 1000 N load cell. ASTM D1621-04a was utilized to determine the compressive modulus and strength of the polyHIPEs.¹⁴ Each polyHIPE specimen was sectioned into three disks (15 mm diameter, 5 mm thickness) using an Isomet saw and compressed at a strain rate of 50 $\mu\text{m/s}$. The compressive modulus was calculated from the slope of the linear region after correcting for zero strain, and the compressive strength was identified as the stress at the yield point or 10% strain, whichever occurred first. Reported moduli and strength data were averages of nine specimens for each composition tested.

Gel Fraction. The gel fraction was measured gravimetrically to evaluate the extent of network formation. After being cured for 24 h, polyHIPE samples were sectioned into 15 mm \times 1 mm disks. The mass was recorded for each specimen after vacuum drying for 48 h, incubating in 100 \times dichloromethane at 20 °C for 48 h, and vacuum drying again until a constant mass was achieved. The final weight divided by the initial weight was assessed as the gel fraction.

Long-Term Storage. Uncured PFDMA HIPEs were stored at 4 °C for up to 6 months and sampled each month to determine the impact of storage on polyHIPE architecture and mechanical properties. After a sample had been removed, it was thawed for 60 min and then injected through a syringe and cured for 48 h prior to characterization, as described above.

In Vitro Cytocompatibility of Macromers. Investigation of macromer cytocompatibility was performed initially prior to seeding cells directly on polyHIPE sections. The *in vitro* cytocompatibility of BDMA, EGDMA, and PFDMA was assessed using a modified ISO 10993-5 extraction dilution test. All macromers were further purified by being washed in deionized water at a volume ratio of 1:100 and incubated under vacuum for 24 h prior to the experiment. Bone marrow-derived hMSCs were obtained as passage 1 in a cryovial from the Center for the Preparation and Distribution of Adult Stem Cells. Cells were cultured in growth medium containing 16.5% fetal bovine serum (Atlanta Biologicals), 1% L-glutamine (Life Technologies), and Minimum Essential Medium α (MEM α , Life Technologies) to 80% confluency and utilized at passages 5 and 6. Cells were trypsinized with 0.25% Trypsin-EDTA (Life Technologies), seeded at a density of 40000 cells/cm² in a 96-well plate, and allowed to adhere for 24 h. The following day, 100 μL of each macromer was incubated in 300 μL of growth medium supplemented with 1 vol % penicillin/streptomycin (Life Technologies) in a 48-well plate to mimic the ratio of organic to aqueous phase in the HIPE. After incubation for 10 min at 37 °C in 5% CO₂, the supernatant above the macromers was aspirated and diluted to 10 \times and 100 \times solutions. This time frame was selected on the basis of the cure rates determined previously for these macromers that approximate the maximal extraction of the unreacted macromer prior to cure. Extracted and diluted media (1 \times , 10 \times , and 100 \times) were then added to cells and the cells cultured for an additional 24 h. Viability was assessed utilizing the Live/Dead assay kit (Molecular Probes). Analysis was completed using a plate reader (Tecan Infinite

M200Pro) with excitation and emission wavelengths of 485 and 528 nm for calcein-AM and 528 and 620 nm for ethidium homodimer-1, respectively. Viability was normalized to cells on tissue culture polystyrene.

In Vitro Cytocompatibility of Redox PolyHIPEs. The viability of hMSCs directly seeded on cured polyHIPEs was assessed to illustrate the cytocompatibility of quick-curing redox foams. PolyHIPEs were fabricated as stated above and sectioned into 500 μm thick wafers using an Isomet saw. Specimens were sterilized for 3 h in 70% ethanol, subjected to a wetting ladder, washed four times with PBS, and incubated overnight in MEM α supplemented with 40% (v/v) FBS at 5% CO_2 and 37 $^\circ\text{C}$. Cells were seeded at densities of 25000 cells/ cm^2 (EGDMA and BDMA) and 100000 cells/ cm^2 (PFDMA) in growth medium supplemented with 1 vol % penicillin/streptomycin and cultured for 3 and 24 h. Viability was assessed using the Live/Dead assay kit. Raster imaging (five images per specimen) was conducted on four specimens ($n = 20$) utilizing a fluorescent microscope (Nikon Eclipse TE2000-S), and cells were manually counted to quantify viability.

Statistical Analysis. The data are displayed as means \pm the standard deviation for each composition. A Student's t test was performed to determine any statistically significant differences between compositions. All tests were conducted a 95% confidence interval ($P < 0.05$).

RESULTS AND DISCUSSION

Effect of Redox Initiator Concentration on Work and Set Time. Prior to curing, all HIPEs flowed like viscous fluids but were rheologically similar to gels ($G' > G''$), which is expected for HIPEs.^{12,15} Their moduli remained relatively constant before curing began, indicating that the emulsions were stable without significant phase separation.¹² Work time is defined by ISO1997 as the “period of time, measured from the start of mixing, during which it is possible to manipulate a dental material without an adverse effect on its properties”, and set time is accepted as the point at which a polymer network is formed.¹² Previously, we reported a cure time for PFDMA of approximately 2 h (5 wt % BPO),⁵ whereas both EGDMA and BDMA require >10 h to set with thermal initiation alone. Utilization of the reducing agent TMA in combination with BPO dramatically reduced work and set times for all materials from hours to minutes. This corresponded to a 1 order of magnitude increase in rate over that for thermal initiation alone.⁵ Increasing the total redox initiator concentration from 0.5 to 5 wt % also decreased both work and set times for all materials (Figure 2). For EGDMA, redox initiation with a concentration of 0.5 wt % decreased the work time to 3.5 min and the set time to 5 min. Increasing the initiator concentration to 1 wt % further decreased the work time to 30 s and the set time to 1 min. BDMA displayed slower set and work times than EGDMA under the same conditions. At 0.5 wt %, BDMA's work time and set time were 5 and 7.5 min, respectively, with further decreases to 1 and 2 min, respectively, at 1.0 wt %. PFDMA had work and set times similar to those of BDMA with (6 and 7 min for 0.1 wt % and 1 and 1.3 min for 1 wt %, respectively). All of the 5 wt % compositions cured before measurements could be taken with the rheometer (<30 s).

PMMA bone cement is one of the most prevalent injectable biomaterials in orthopedic applications because it undergoes a transition from a low-viscosity liquid to a rigid solid within 15 min.^{16–19} The PMMA physical transition allows surgeons to work with either a liquid or putty to best suite their procedure and is a contributing factor in PMMA's widespread use.¹⁸ The findings from this study demonstrate the utility of the redox system for increasing the cure rate of the polyHIPEs to ranges

comparable to those of PMMA bone cements. We also demonstrated that the cure rate can be further modulated from <30 s to 10 min by changing the redox initiator concentration. In contrast to PMMA, which is nonporous, nonbiodegradable, and highly exothermic with peak temperatures reaching 110 $^\circ\text{C}$,²⁰ these polyHIPEs cure to porous and degradable materials with a maximal exotherm of only 42 $^\circ\text{C}$. This low exotherm would be critical if the scaffolds were to be used synergistically with stem cells or growth factors. It should be noted that *in vivo* polymerization may occur more rapidly if the mixing head temperature is elevated to 37 $^\circ\text{C}$, causing the HIPE to warm quicker than tested. This effect is expected to be minimal given that the HIPE passes through the mixing head for <1 s. If differences were found and needed to be adjusted, this work demonstrates that set time can be increased by decreasing the total amount of initiator or decreasing the reducing initiator concentration.

Effect of Redox Initiator Concentration on Network Formation. Additional rheological and gel fraction data were analyzed to investigate the impact of redox initiation concentration on network formation in candidate polyHIPEs. In each material, an induction period was evident prior to an increase in modulus that was dependent on macromer chemistry (EGDMA $<$ BDMA $<$ PFDMA) that was primarily responsible for the difference in cure times (Figure 2). It was hypothesized that reduced radical diffusion and steric hindrances associated with an increased macromer molecular weight resulted in longer induction periods, especially at the low-initiator concentration compositions.²¹ PFDMA, BDMA, and EGDMA have molecular masses of ~ 362 , 226, and 198 g/mol, respectively. HIPE viscosity trended with macromer molecular weight, with the value of PFDMA almost 30 times greater than that of EGDMA. The increased viscosity likely inhibited initiator diffusion and reaction in the PFDMA HIPEs as compared to those in the EGDMA HIPEs.^{21,22} As the initiator concentration was increased from 0.5 to 1.0 wt %, this induction period decreased and the slopes of the moduli increased, suggesting an increased polymerization rate.²³ This was attributed to an increased number of initiation sites leading to more chains growing simultaneously and causing chain molecular weight to increase more rapidly.

The gel fraction (Table 1) was utilized to compare the extent of network formation in polyHIPEs after they had been cured for 24 h and ranged from 78 to 92% for all compositions (Table 1). As expected, an increasing initiator concentration correlated with an increased gel fraction. The PFDMA gel fraction increased the most from 78 to 86%. The BDMA gel fraction also increased significantly with higher initiator concentrations (from 86 to 92%), whereas the EGDMA gel fractions increased only from 86 to 89%. Both EGDMA and BDMA had gel fractions significantly higher than those of the corresponding PFDMA polyHIPEs, likely because of steric hindrance and a reduced rate of radical diffusion associated with its higher molecular weight. Additionally, highly cross-linked microgels could form and begin to sterically hinder further cross-linking, increasing the number of network defects and free ends.²¹ It should be noted that PGPR was not removed from the specimens prior to DCM incubation and should account for approximately 9% of specimen mass. Fourier transform infrared spectroscopy of the extract solutions showed the presence of PGPR, but the concentration was not quantified (data not shown). Assuming all of the PGPR was removed with the DCM, gel fractions were actually between 94 and 100%.

Table 1. Effects of Macromer and Initiator Chemistry on Average Gel Fractions, Pore Diameters, and Interconnect Diameters of Various PolyHIPE Formulations

material	redox initiator (wt %)	gel fraction (%)	pore diameter (μm)	interconnect diameter (μm)
EGDMA	0.5	86.1 \pm 2.8	27 \pm 12 ^a	3 \pm 2
	1.0	89.1 \pm 0.5	20 \pm 10	3 \pm 1
	5.0	89.0 \pm 1.0	19 \pm 12	3 \pm 1
BDMA	0.5	85.8 \pm 0.4	14 \pm 6	3 \pm 1
	1.0	89.3 \pm 0.4	14 \pm 6	3 \pm 1
	5.0	92.1 \pm 0.3	13 \pm 7 ^b	2 \pm 1
PFDMA	0.5	77.9 \pm 1.7	5 \pm 3 ^c	1 \pm 1
	1.0	81.0 \pm 0.8	6 \pm 3	1 \pm 1
	5.0	85.6 \pm 0.8	6 \pm 3	1 \pm 1

material	TMA:BPO (wt %:wt %)	gel fraction (%)	pore diameter (μm)	interconnect diameter (μm)
EGDMA	0.5:1.0	87.8 \pm 0.7	19 \pm 8	3 \pm 1
	1.0:1.0	89.1 \pm 0.5	20 \pm 10 ^d	3 \pm 1
	5.0:1.0	86.5 \pm 1.9	17 \pm 11	2 \pm 1

^a $P < 0.001$ compared to EGDMA 1.0 and 5.0 wt % pore sizes. ^b $P < 0.05$ compared to BDMA 0.5 and 1.0 wt % pore sizes. ^c $P < 0.01$ compared to PFDMA 1.0 and 5.0 wt % pore sizes. ^d $P < 0.01$ compared to 0.5:1.0 and 5.0:1.0 TMA:BPO pore sizes.

Overall, these polyHIPEs showed excellent network formation that was further enhanced at higher initiator concentrations.

Effect of Redox Initiator Concentration and Storage on Pore Architecture. The impact of the rapid, redox-initiated cure on polyHIPE microarchitecture was examined to ensure retention of desirable pore size and interconnection. EGDMA polyHIPEs possessed the largest pore diameters, almost double the size of BDMA pores and quadruple the size of PFDMA pores at each initiator concentration. Traditionally, pore size has been used as a marker of emulsion stability, with a

smaller pore size indicating enhanced stability and reduced droplet coalescence prior to the gel point.^{24,25} In this study, an increasing pore size correlated with a decreasing HIPE viscosity: PFDMA (11.0 Pa s), BDMA (0.464 Pa s), and EGDMA (0.343 Pa s). This was consistent with the previous literature reports of increased emulsion viscosity impeding droplet coalescence and resulting in smaller pores.⁹ Despite differences between materials, scanning electron micrographs revealed that the average pore and interconnect diameter were not affected by the redox initiator concentration for most materials (Figure 3 and Table 1). The 0.5% EGDMA was the exception with an average pore size of 26 μm , significantly larger than that of the 1.0 and 5.0% polyHIPEs (20 μm) and indicative that some amount of coalescence occurred prior to the gel point. The rapid cure of both the 1.0 and 5.0 wt % EGDMA polyHIPEs reduced droplet coalescence, and thus, no change in pore size was observed.

Although there are no clear targets for ideal pore diameters to regenerate tissues, these pore sizes are relatively small compared to the general goal of $>100 \mu\text{m}$; however, recent studies indicate that $<40 \mu\text{m}$ pores improve regeneration.^{26,27}

We have previously demonstrated that the emulsion composition and processing can be modified to increase or decrease the pore diameter. Future studies to increase the pore size of these grafts will utilize established techniques of decreasing surfactant concentration and incorporating additives such as poly(ethylene glycol).^{5,7,25,28} BDMA and EGDMA polyHIPEs possessed pore diameters of up to 60 μm when the polyHIPEs were cured via thermal initiation (data not shown). We hypothesized that the use of the static mixing head in this study decreased the pore size by imparting extra shear forces on the emulsion and further breaking droplets down to smaller diameters. Therefore, the use of a large diameter mixing head should minimize the impact on pore diameter for all materials and compositions tested.

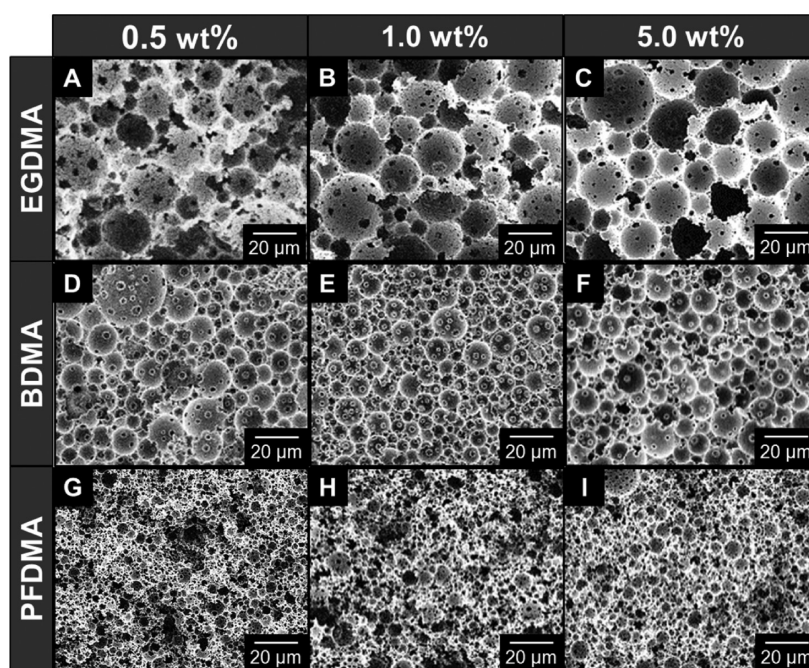


Figure 3. Representative SEMs illustrating the effect of initiator concentration on the pore architecture of EGDMA (A–C), BDMA (D–F), and PFDMA (G–I) polyHIPEs.

A crucial element of the double-barrel system is that the two HIPEs can be stored separately until they are needed, and the shelf life can be further extended by storage at reduced temperatures. PFDMA HIPEs were stored at 4 °C with samples removed and cured to examine any effect of storage on pore size, indicating droplet coalescence or phase separation over time. No significant change in pore architecture was observed over a period of 6 months (Figure 4). This same technique

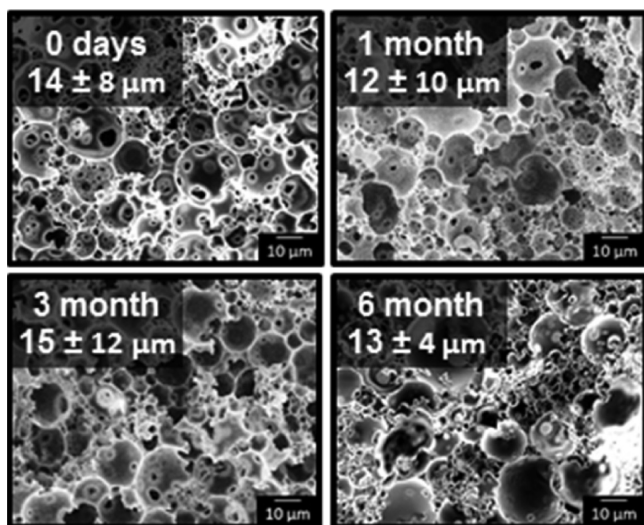
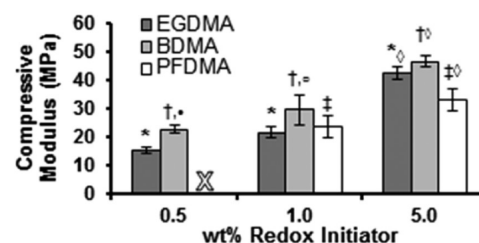


Figure 4. Representative SEMs of PFDMA polyHIPEs after the storage of unpolymerized HIPEs at 4 °C for up to 6 months.

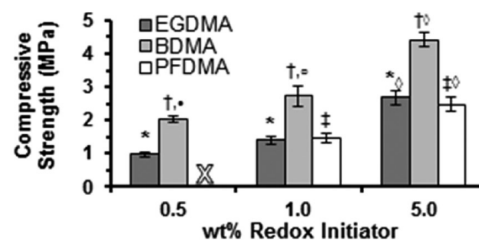
could be used with any emulsion but is especially useful for these solvent-free polyHIPEs that could encapsulate live cells or other biological therapeutics that could then be cryogenically stored without losing efficacy. Also, this method could facilitate scale-up with a central facility making the emulsion-filled syringes and transported to facilities where needed.

Effect of Redox Initiator Concentration on Compressive Properties. The compressive modulus and strength are clinically important for bone grafts in stabilizing defects. An increased defect stability would reduce the necessity for immobilization and allow for earlier loading, which has established benefits in stimulating bone regeneration.²⁹ Although the polyHIPEs set within several minutes, specimens were sectioned after a 24 h cure for further characterization. The compressive modulus and strength increased as the redox initiator concentration increased for all materials tested (Figure 5). BDMA was significantly stiffer and stronger than both EGDMA and PFDMA at each concentration tested. These differences in strength were more pronounced than those of the modulus, with even the weakest BDMA (0.5 wt % initiator) having a yield strength higher than those of all but the strongest EGDMA and PFDMA polyHIPEs (5.0 wt % initiator). The 0.5 wt % PFDMA samples were not tested in compression because they possessed large regions of uncured HIPE (reflected in their lower gel fraction). We hypothesize that the high viscosity of PFDMA decreased the mixing efficiency of the two HIPEs and limited radical diffusion resulting in regions of uncured HIPEs. This was not observed in the 1.0 or 5.0% PFDMA HIPEs because of the higher concentration of the initiator that limited the role of radical diffusion throughout the material. A longer static mixing head may eliminate the uncured regions in the 0.5% redox PFDMA. Representative loading curves are

A) PolyHIPE Compressive Modulus



B) PolyHIPE Compressive Strength



*: P < 0.01 compared to all BDMA polyHIPEs
 †: P < 0.01 compared to all EGDMA polyHIPEs
 ‡: P < 0.01 compared to all PFDMA polyHIPEs
 •: P < 0.01 compared to all 0.5 wt% polyHIPEs
 ◦: P < 0.01 compared to all 1.0 wt% polyHIPEs
 ◊: P < 0.01 compared to all 5.0 wt% polyHIPEs

Figure 5. Effect of initiator concentration on compressive modulus (A) and strength (B) for each material. One composition had large regions of uncured material and was not tested, denoted with an X.

presented in Figure 6. EGDMA polyHIPEs were brittle and reduced to a compacted powder after compressive testing, whereas both BDMA and PFDMA retained their dimensions. The toughness for all materials appeared to increase at higher initiator concentrations, with 5 wt % redox BDMA and PFDMA specimens showing no signs of brittle fracture.

These porous materials approach the compressive properties of cancellous bone when matched by density, indicating the potential to mechanically stabilize the defect and elicit the appropriate mechanical cues to regenerate bone.^{2,30,31} Furthermore, some studies have shown that the mechanical properties required to trigger bone formation may be much lower than those of fully matured bone tissue.¹⁷ In addition, the redox initiator system in these studies resulted in a rapid maturation of mechanical properties compared to that of thermal initiation alone. Previously, the compressive modulus and strength of PFDMA polyHIPEs thermally cured with 5 wt % BPO increased over a 2 week incubation at 37 °C (Figure 7). In that time, the modulus increased from 8.5 to 43 MPa and the strength from 0.4 to 3 MPa. In contrast, the 5 wt % redox PFDMA polyHIPEs achieved similar properties within 24 h of incubation and remained constant for the 2 weeks tested. As such, the redox system could potentially be used as an immediate fixation device and/or allow patients to begin loading the injury site more quickly, which can improve patient outcomes.²⁹

Effect of the TMA:BPO Ratio on PolyHIPE Properties.

The ratio of reductant to oxidant was also investigated to decouple the effects of rapid curing rates from increased initiator concentration. As expected, increasing the relative amount of TMA to BPO resulted in decreased work and set times, from 90 to 30 s and from 2.5 to 1 min, respectively (Figure 8A). It should be noted that the 5.0 wt % TMA/1.0 wt

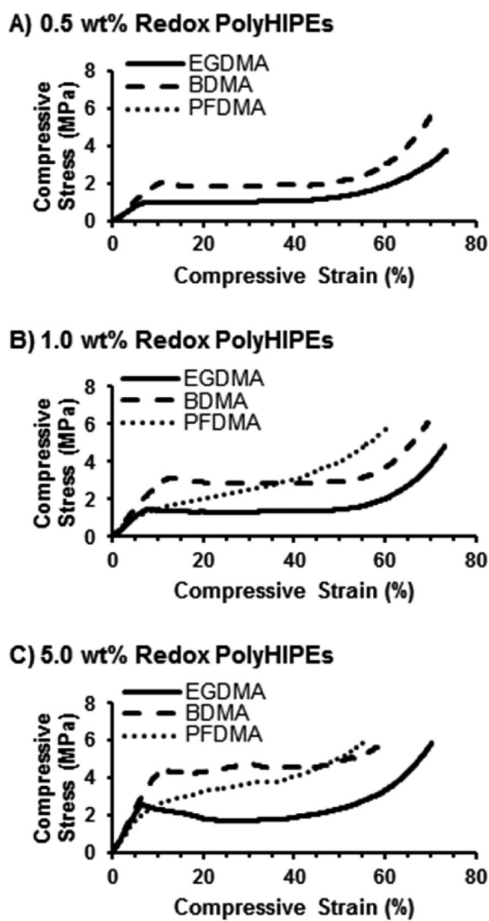


Figure 6. Representative compressive loading curves for each material and initiator concentration.

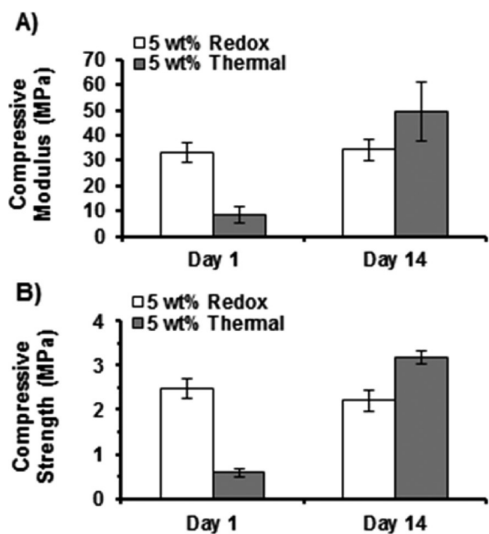


Figure 7. Effect of incubation for 1 and 14 days at 37 °C on PFDMA polyHIPE compressive (A) modulus and (B) strength.

% BPO HIPE set before testing could begin (<20 s). We hypothesize that increasing the relative amount of TMA increases its availability to react with BPO, resulting in faster radical production and initiation. Other researchers have shown similar results with BPO/TMA systems and identified the formation of the BPO–TMA complex as the rate-limiting step in radical production.^{32,33} As such, the faster initiation would

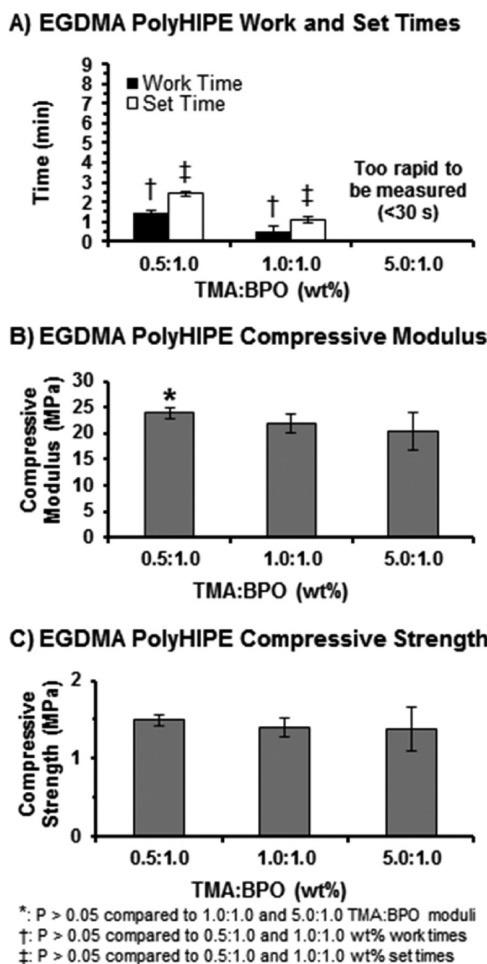


Figure 8. Effect of an increasing TMA:BPO ratio in EGDMA polyHIPEs on (A) work and set times, (B) the compressive modulus, and (C) the compressive strength.

allow the HIPEs to form a network more quickly and increase the cure rate. The compressive data collected after 24 h indicated that the redox initiator ratio had little to no effect on the compressive modulus or strength (Figure 8B,C). There was also a minimal effect on the pore architecture. The average pore diameter varied slightly as the relative amount of TMA was increased, but no clear trend was observed. The 1.0:1.0 ratio had the largest average pore diameter (20 μm), with 0.5 and 5.0:1.0 ratios yielding slightly smaller values of 19 and 17 μm , respectively. Although statistically significant, these differences are small, and the overall pore architecture is similar between the compositions.

Overall, these results demonstrate that the polyHIPE work and set time can be tuned in a manner independent of other polyHIPE properties (compressive modulus and strength, pore and interconnect diameter) with small variations in the reductant:oxidant ratio. For biomedical devices, especially tissue-engineered grafts, this provides researchers a route for preserving graft physical properties and cytocompatibility while optimizing work and set times to meet physician preferences.

In Vitro hMSC Cytocompatibility Assessment. Initial studies of the surfactant PGPR confirmed that there were no cytotoxic effects (>95% viability) after direct cellular exposure of the surfactant at concentrations used in these studies. Assessment of hMSC viability was then performed after exposure to extract medium from unreacted macromers and

direct seeding onto cured polyHIPE grafts. Given the proposed application as an injectable bone graft, the unreacted macromer study provides an initial assessment of the effect of a brief exposure of the macromer to cells prior to cross-linking *in situ*. The viability of hMSCs after exposure to PFDMA extract medium was positive (>80%), whereas the viability decreased significantly after exposure to EGDMA and BDMA extract media (Figure 9). Tenfold and 100-fold dilution of the extract

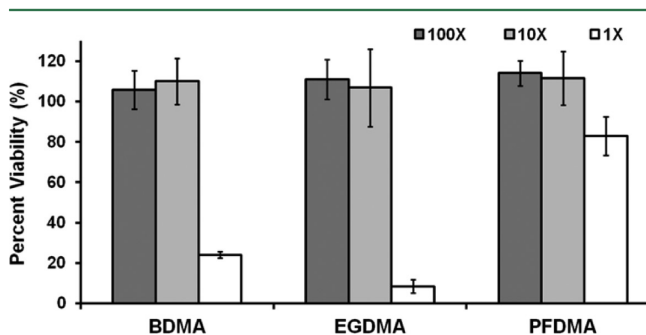


Figure 9. hMSC viability after a 24 h incubation with diluted extracts (1X, 10X, and 100X) from 10 min incubations of medium with each macromer.

medium resulted in a large viability for all macromers. Despite the similar low viability of unsaturated macromer extracts (<5% viability), Mistry et al. reported no adverse inflammatory response or necrosis after implantation of the polymer in a bone defect.^{34,35} Next, direct seeding on the cross-linked polyHIPE grafts was evaluated to determine the potential of these network structures to support hMSC adhesion and viability. Cell viability results of all three macromers were greater than 80% at 24 h, which is generally considered to be cytocompatible (Figure 10). Future studies will focus on the PFDMA macromer as being the most promising in terms of cytocompatibility and will assess the cytocompatibility of degradation products using a transwell setup and longer time points. Given the similarity of expected degradation products to previously tested fumarate-based bone grafts, we do not anticipate any issues with these studies.^{34–36}

CONCLUSIONS

This study demonstrates the benefits of redox-initiated polyHIPEs delivered using double-barrel syringes as tissue-engineered bone grafts. Redox initiation reduced work and set times from hours to minutes, matching those of current products like PMMA bone cement. These reduced cure times were also achieved with lower total initiator concentrations that may enhance material cytocompatibility. Increasing the redox initiator concentration increased the compressive modulus and strength with a minimal impact on the pore architecture. Further modulation of the reductant:oxidant ratio decoupled the set time from the compressive modulus and strength, allowing for increased tunability of future scaffold properties. The use of the double-barrel syringe permitted the emulsions to be stored for months at reduced temperatures and then undergo rapid on-demand curing upon injection due to mixing of the two components. Overall, the methodology developed in these studies facilitates clinical translation of this technology by providing new graft materials with improved attributes that maintain similar handling and deployment of traditional PMMA bone cements.

AUTHOR INFORMATION

Corresponding Author

*E-mail: cosgriff.hernandez@tamu.edu.

Present Address

†P.D.: Department of Biomolecular Engineering, University of California, Santa Cruz, CA 95064.

Notes

The authors declare no competing financial interest.

ACKNOWLEDGMENTS

Funding was provided by National Institutes of Health Grant R21 AR057531. We acknowledge Palsgaard USA for providing PGPR 4125. Undergraduate student support was provided by Undergraduate Student Research Grants from Texas A&M University.

REFERENCES

(1) Middleton, J. C.; Tipton, A. J. Synthetic biodegradable polymers as orthopedic devices. *Biomaterials* **2000**, *21* (23), 2335–2346.

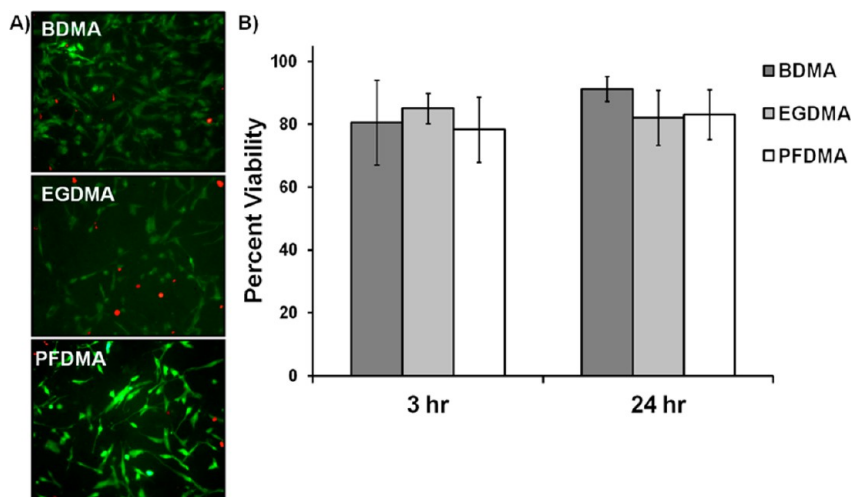


Figure 10. hMSC viability after 3 and 24 h directly seeded on BDMA, EGDMA, and PFDMA 1% redox polyHIPE sections. (A) Micrographs illustrating live (green) and dead (red) cells on the respective polyHIPE sections at 24 h. (B) Viability of cells at each time point ($n = 20$).

- (2) Karageorgiou, V.; Kaplan, D. Porosity of 3D biomaterial scaffolds and osteogenesis. *Biomaterials* **2005**, *26*, 5474–5491.
- (3) Peter, S. J.; Miller, M. J.; Yasko, A. W.; Yaszemski, M. J.; Mikos, A. G. Polymer concepts in tissue engineering. *J. Biomed. Mater. Res.* **1998**, *43* (4), 422–427.
- (4) Akay, G.; Birch, M. A.; Bokhari, M. A. Microcellular polyHIPE polymer supports osteoblast growth and bone formation in vitro. *Biomaterials* **2004**, *25*, 3991–4000.
- (5) Moglia, R. S.; Holm, J. L.; Sears, N. A.; Wilson, C. J.; Harrison, D. M.; Cosgriff-Hernandez, E. Injectable PolyHIPEs as High-Porosity Bone Grafts. *Biomacromolecules* **2011**, *12* (10), 3621–3628.
- (6) Moglia, R. S.; Robinson, J. L.; Muschenborn, A. D.; Touchet, T. J.; Maitland, D. J.; Cosgriff-Hernandez, E. Injectable polyMIPE scaffolds for soft tissue regeneration. *Polymer* **2014**, *55*, 426–434.
- (7) Robinson, J. L.; Moglia, R. S.; Stuebben, M. C.; McEnery, M. A. P.; Cosgriff-Hernandez, E. Achieving interconnected pore architecture in injectable polyHIPEs for bone tissue engineering. *Tissue Eng, Part A* **2014**, *20* (5–6), 1103–1112.
- (8) Hou, Q.; De Bank, P. A.; Shakesheff, K. M. Injectable scaffolds for tissue regeneration. *J. Mater. Chem.* **2004**, *14*, 1915–1923.
- (9) Butler, R.; Hopkinson, I.; Cooper, A. I. Synthesis of porous emulsion-templated polymers using high internal phase CO₂-in-water emulsions. *J. Am. Chem. Soc.* **2003**, *125* (47), 14473–14481.
- (10) Wu, R.; Menner, A.; Bismarck, A. Macroporous polymers made from medium internal phase emulsion templates: Effect of emulsion formulation on the pore structure of polyMIPEs. *Polymer* **2013**, *54*, 5511–5517.
- (11) Timmer, M. D.; Horch, A. R.; Ambrose, C. G.; Mikos, A. G. Effect of physiological temperature on the mechanical properties and network structure of biodegradable poly(propylene fumarate)-based networks. *J. Biomater. Sci., Polym. Ed.* **2003**, *14* (4), 369–382.
- (12) Foudazi, R.; Gokun, P.; Feke, D. L.; Rowan, S. J.; Manas-Zloczower, I. Chemorheology of poly(high internal phase emulsions). *Macromolecules* **2013**, *46* (13), 5393–5396.
- (13) Barbetta, A.; Cameron, N. R. Morphology and surface area of emulsion-derived (PolyHIPE) solid foams prepared with oil-phase soluble porogenic solvents: Span 80 as surfactant. *Macromolecules* **2004**, *37*, 3188–3201.
- (14) Standard test method for compressive properties of rigid cellular plastics (D 1621-04a); ASTM International: West Conshohocken, PA, 2004 (D 1621-04a).
- (15) Mason, T. G.; Lacasse, M.-D.; Grest, G. S.; Levine, D.; Bibette, J.; Weitz, D. A. Osmotic pressure and viscoelastic shear moduli of concentrated emulsions. *Phys. Rev. E* **1997**, *56* (3), 3150–3166.
- (16) Stryker HydroSet injectable HA bone substitute. <http://www.stryker.com>.
- (17) Temenoff, J. S.; Mikos, A. G. Injectable biodegradable materials for orthopedic tissue engineering. *Biomaterials* **2000**, *21*, 2405–2412.
- (18) Farrar, D. F.; Rose, J. Rheological properties of PMMA bone cements during curing. *Biomaterials* **2001**, *22* (22), 3005–3013.
- (19) Neurotherm Bone cement products. <http://www.parallaxmed.com>.
- (20) McMahon, S.; Hawdon, G.; Bare, J.; Sim, Y.; Bertollo, N.; Walsh, W. R. Thermal necrosis and PMMA: A cause for concern? *J. Bone Jt. Surg., Br. Vol.* **2012**, *94-B* (Suppl. XXIII), 64.
- (21) Chiu, Y. Y.; Lee, L. J. Microgel formation in the free radical crosslinking polymerization of ethylene glycol dimethacrylate (EGDMA). I. Experimental. *J. Polym. Sci., Part A: Polym. Chem.* **1995**, *33* (2), 257–267.
- (22) Goodner, M. D.; Bowman, C. N. Modeling Primary Radical Termination and Its Effects on Autoacceleration in Photopolymerization Kinetics. *Macromolecules* **1999**, *32* (20), 6552–6559.
- (23) Van Assche, G.; Verdonck, E.; Van Mele, B. Interrelations between mechanism, kinetics, and rheology in an isothermal cross-linking chain-growth copolymerisation. *Polymer* **2001**, *42* (7), 2959–2968.
- (24) Christenson, E. M.; Soofi, W.; Holm, J. L.; Cameron, N. R.; Mikos, A. G. Biodegradable Fumarate-Based PolyHIPEs as Tissue Engineering Scaffolds. *Biomacromolecules* **2007**, *8* (12), 3806–3814.
- (25) Williams, J. M.; Gray, A. J.; Wilkerson, M. H. Emulsion stability and rigid foams from styrene or divinylbenzene water-in-oil emulsions. *Langmuir* **1990**, *6*, 437–444.
- (26) Hulbert, S. F.; Young, F. A.; Mathews, R. S.; Klawitter, J. J.; Talbert, C. D.; Stelling, F. H. Potential of ceramic materials as permanently implantable skeletal prostheses. *J. Biomed. Mater. Res.* **1970**, *4*, 433–456.
- (27) Madden, L. R.; Mortisen, D. J.; Sussman, E. M.; Dupras, S. K.; Fugate, J. A.; Cuy, J. L.; Hauch, K. D.; Laflamme, M. A.; Murry, C. E.; Ratner, B. D. Proangiogenic scaffolds as functional templates for cardiac tissue engineering. *Proc. Natl. Acad. Sci. U.S.A.* **2010**, *107* (34), 15211–15216.
- (28) Williams, J. M. High internal phase water-in-oil emulsions: Influence of surfactants and cosurfactants on emulsion stability and foam quality. *Langmuir* **1991**, *7*, 1370–1377.
- (29) Munin, M. C.; Rudy, T. E.; Glynn, N. W.; Crossett, L. S.; Rubash, H. E. Early inpatient rehabilitation after elective hip and knee arthroplasty. *JAMA, J. Am. Med. Assoc.* **1998**, *279* (11), 847–852.
- (30) Coombes, A. G. A.; Meikle, M. C. Resorbable synthetic polymers as replacements for bone graft. *Clin. Mater.* **1994**, *17* (1), 35–67.
- (31) Svaldi-Muggli, D.; Burkoth, A. K.; Anseth, K. S. Crosslinked polyanhydrides for use in orthopaedic applications: Degradation behavior and mechanics. *J. Biomed. Mater. Res.* **1999**, *46*, 271–278.
- (32) Sideridou, I. D.; Achilias, D. S.; Karava, O. Reactivity of benzoyl peroxide/amine system as an initiator for the free radical polymerization of dental and orthopaedic dimethacrylate monomers: Effect of the amine and monomer chemical structure. *Macromolecules* **2006**, *39* (6), 2072–2080.
- (33) Pryor, W. A.; Hendrickson, W. H., Jr. The mechanism of radical production from the reaction of N,N-dimethylaniline with benzoyl peroxide. *Tetrahedron Lett.* **1983**, *24* (14), 1459–1462.
- (34) Mistry, A.; Pham, Q.; Schouten, C.; Yeh, T.; Christensen, E.; Mikos, A.; Jansen, J. *In vivo* bone biocompatibility and degradation of porous fumarate-based polymer/alumoxane nanocomposites for bone tissue engineering. *J. Biomed. Mater. Res., Part A* **2010**, *92A* (2), 451–462.
- (35) Mistry, A. S.; Mikos, A. G.; Jansen, J. A. Degradation and biocompatibility of a poly(propylene fumarate)-based/alumoxane nanocomposite for bone tissue engineering. *J. Biomed. Mater. Res., Part A* **2007**, *83A*, 940–953.
- (36) Timmer, M. D.; Shin, H.; Horch, A. R.; Ambrose, C. G.; Mikos, A. G. In vitro cytotoxicity of injectable and biodegradable poly(propylene fumarate)-based networks: Unreacted macromers, cross-linked networks, and degradation products. *Biomacromolecules* **2003**, *4*, 1026–1033.